

SIGLEC15, negatively correlated with PD-L1 in HCC, could induce CD8+ T cell apoptosis to promote immune evasion

Zheng Chen^{a*}, Mincheng Yu^{a*}, Bo Zhang^{a*}, Lei Jin^a, Qiang Yu^a, Shuang Liu^b, Binghai Zhou^c, Jiuliang Yan^d, Wentao Zhang^a, Xiaoqiang Li^e, Yongfeng Xu^a, Yongsheng Xiao^a, Jian Zhou^a, Jia Fan^a, Mien-Chie Hung^{f,g}, Qinghai Ye^a, Hui Li^{a,h}, and Lei Guo^a

^aDepartment of Liver Surgery and Transplantation, Liver Cancer Institute, Zhongshan Hospital, Fudan University, Key Laboratory of Carcinogenesis and Cancer Invasion, Ministry of Education, Shanghai, P.R. China; ^bNeurosurgery Department of Zhongshan Hospital, Fudan University, Shanghai, P.R. China; ^cDepartment of Hepatobiliary and Pancreatic Surgery, The Second Affiliated Hospital of Nanchang University, Nanchang, P.R. China; ^dDepartment of Pancreatic Surgery, Shanghai General Hospital and Shanghai Key Laboratory of Pancreatic Disease, Institute of Pancreatic Disease, Shanghai Jiao Tong University School of Medicine, Shanghai, P.R. China; ^eDepartment of Thoracic Surgery, Peking University Shenzhen Hospital, Shenzhen, P.R. China; ^fGraduate Institute of Biomedical Sciences, Research Center for Cancer Biology and Center for Molecular Medicine, China Medical University, Taichung, TX, Taiwan; ^gDepartment of Molecular and Cellular Oncology, The University of Texas MD Anderson Cancer Center, Houston, TX, USA; ^hShanghai Medical College and Zhongshan Hospital Immunotherapy Translational Research Center, Shanghai, P.R. China

ABSTRACT

Functional roles of SIGLEC15 in hepatocellular carcinoma (HCC) were not clear, which was recently found to be an immune inhibitor with similar structure of inhibitory B7 family members. SIGLEC15 expression in HCC was explored in public databases and further examined by PCR analysis. SIGLEC15 and PD-L1 expression patterns were examined in HCC samples through immunohistochemistry. SIGLEC15 expression was knocked-down or over-expressed in HCC cell lines, and CCK8 tests were used to examine cell proliferative ability in vitro. Influences of SIGLEC15 expression on tumor growth were examined in immune deficient and immunocompetent mice respectively. Co-culture system of HCC cell lines and Jurkat cells, flow cytometry analysis of tumor infiltrated immune cells and further sequencing analyses were performed to investigate how SIGLEC15 could affect T cells in vitro and in vivo. We found SIGLEC15 was increased in HCC tumor tissues and was negatively correlated with PD-L1 in HCC samples. In vitro and in vivo models demonstrated inhibition of SIGLEC15 did not directly influence tumor proliferation. However, SIGLEC15 could promote HCC immune evasion in immune competent mouse models. Knock-out of *Siglec15* could inhibit tumor growth and reinvigorate CD8+ T cell cytotoxicity. Anti-SIGLEC15 treatment could effectively inhibit tumor growth in mouse models with or without mononuclear phagocyte deletion. Bulk and single-cell RNA sequencing data of treated mouse tumors demonstrated SIGLEC15 could interfere CD8+ T cell viability and induce cell apoptosis. In all, SIGLEC15 was negatively correlated with PD-L1 in HCC and mainly promote HCC immune evasion through inhibition of CD8+ T cell viability and cytotoxicity.

ARTICLE HISTORY

Received 27 April 2024
Revised 11 June 2024
Accepted 1 July 2024

KEYWORDS

Immune checkpoints;
immune evasion; liver
cancer; survival signaling;
tumor microenvironment

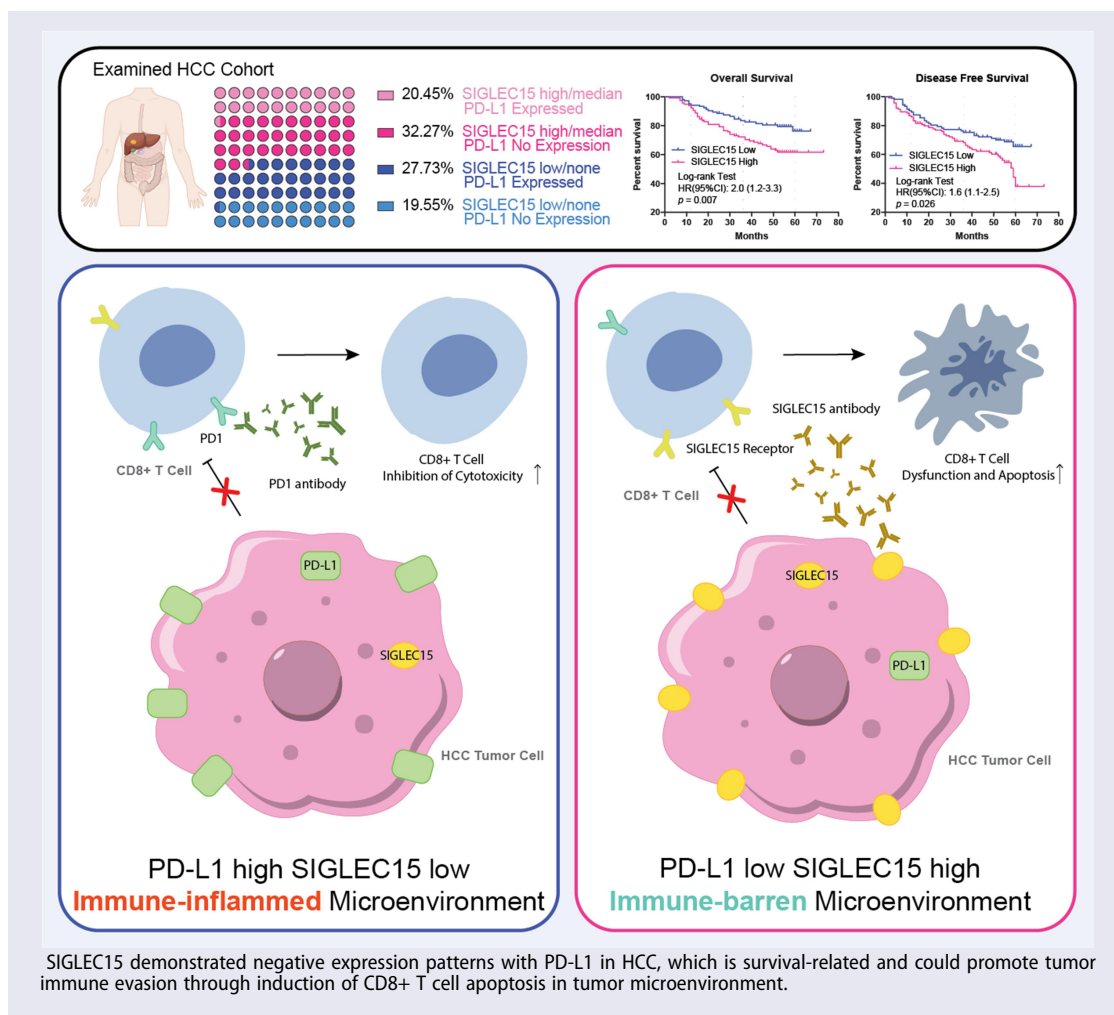
CONTACT Mien-Chie Hung  mhung@cmu.edu.tw  Graduate Institute of Biomedical Sciences, Research Center for Cancer Biology and Center for Molecular Medicine, China Medical University, #100, Sec. 1, Jingmao Rd. Beitun District, Taichung 406, Taiwan; Qinghai Ye  ye.qinghai@zs-hospital.sh.cn; Lei Guo  guo.lei@zs-hospital.sh.cn; Hui Li  li.hui1@zs-hospital.sh.cn  Department of Liver Surgery and Transplantation, Liver Cancer Institute, Zhongshan Hospital, Fudan University, Key Laboratory of Carcinogenesis and Cancer Invasion, Ministry of Education, No. 180 Fenglin Road, Xuhui District, Shanghai 200032, China

*Zheng Chen, Mincheng Yu and Bo Zhang contributed equally to the manuscript.

 Supplemental data for this article can be accessed online at <https://doi.org/10.1080/2162402X.2024.2376264>

© 2024 The Author(s). Published with license by Taylor & Francis Group, LLC.

This is an Open Access article distributed under the terms of the Creative Commons Attribution-NonCommercial License (<http://creativecommons.org/licenses/by-nc/4.0/>), which permits unrestricted non-commercial use, distribution, and reproduction in any medium, provided the original work is properly cited. The terms on which this article has been published allow the posting of the Accepted Manuscript in a repository by the author(s) or with their consent.



Introduction

Hepatocellular carcinoma (HCC) is one of the leading causes for cancer-associated death worldwide.^{1,2} Fifty percent of patients afflicted by HCC experience early recurrence after surgery, and the overall response to chemotherapy is not satisfied.³ Although immunotherapy targeting PD-1/PD-L1 or CTLA-4 axis has achieved success in some patients, the objective response rate for HCC ranges from 15–20%, which has led to the exploration of combining therapy or additional targets in order to increase immunotherapy efficacy in patients with limited results.^{4–8}

PD1 and CTLA-4 are both B7 family members, which played vital roles in immune regulation, and a series of studies tried to screen other B7 family members as potential immune regulators, which could be targets to ‘tip-off’ immune exhaustion in cancer treatment.^{9–12} SIGLEC15, expressed by macrophages, has recently been reported to share a similar genetic sequence and protein structure with inhibitory B7 family members and could suppress CD8+ T cell function in melanoma, which was formerly reported to be involved in bone resorption, immune defenses and inflammation.^{13–16} Liver cancer otherwise has been considered to have a suppressive immune microenvironment with unique immune cell populations, metabolic changes and intrinsic oncogenic signals.^{17–21} The expression

patterns and immunoregulatory roles of SIGLEC15 in HCC have not been elucidated, and in our investigation, we found that SIGLEC15 was negatively correlated with PD-L1 expression in HCC samples, relating an immune-barren microenvironment. Tumor-derived SIGLEC15 did not directly impact tumor growth; rather, it could lead to tumor immune evasion through induction of cytotoxic CD8+ T cell apoptosis, which could be redirected and reduced by anti-SIGLEC15 treatment. The preclinical results of our study provided rationale for precision immunotherapy in treatment of advanced HCC.

Methods

Reverse transcript quantitative polymerase chain reaction (RT – qPCR) analysis

Total RNA of transfected cell lines was extracted with TRI reagent (Sigma) according to manufactured protocols, and then chloroform and isopropanol were respectively used to filter procured total RNA through centrifugation at 10,000 rpm for 10 min. Tumor tissue was frozen in liquid nitrogen and then put into 1.5 ml tubes with grinding beads, which were filled with 1 ml TRI reagent (Sigma); afterward, tissues were grand at a frequency of 60 Hz for 30s to get total

RNA before centrifugation. Master Mix (TAKARA) was used to generate complementary DNA for PCR analysis according to the protocols, and finally, SYBR GREEN (TAKARA) kit was used for RT – qPCR analysis of the quantitated cDNA solution. Primers for targeted genes were generated by GenePharma (China) (Table S4).

Western-blot analysis (WB)

Cell samples were washed with iced PBS for 3 times, and then NP40, containing proteinase inhibitors, was used for cell lysis. Yielded cell lysate was then loaded for centrifugation at 10,000 rpm for 10 min at 4°C to get rid of the cell debris. Protein buffer was firstly examined by BCA kit to estimate the protein concentration of each sample, after which cell lysates were added into each cell of prepared gels for electrophoresis (300 mA, 30 min). Afterwards, separated proteins in gel were transferred onto PVDF membranes (45 µm, Millipore) through wet transfer method (120 V, 1.5 h). The whole membrane was then blocked with QuickBlock Western solution (Beyotime P0252) for 15 min. Membranes were trimmed according to the respective molecular weights of targeted genes, and then trimmed membrane lanes were for each primary antibody incubation (4°C, overnight; SIGLEC15 1:1000; PD-L1 1:1000) (Table S2). Before further incubation with secondary antibodies (room temperature, 30 min), membrane lanes were washed twice with TBST. Immobilon Western HRP Substrate (Millipore) was used for exposure detection.

Cell lines and genetic modification

The cell lines of L02 (RRID: CVCL_6926), HepG2 (RRID: CVCL_0027), Hep3B (RRID: CVCL_0326), PLC (RRID: CVCL_0485), HCCLM3 (RRID: CVCL_6832), Huh7 (RRID: CVCL_0036), HCC7721 (RRID: CVCL_0534), MHCC97H (RRID: CVCL_4972), MHCC97L (RRID: CVCL_4973) and Hep1–6 (RRID: CVCL_0327) used in our investigation were provided by the Liver Cancer Institute of Zhongshan Hospital, affiliated with Fudan University, Shanghai, China. The Jurkat cell line (RRID: CVCL_0065) was purchased from GeneChem (China). Lentiviruses targeting human SIGLEC15 were generated by GeneChem (China); plasmids for human SIGLEC15 over-expression and Cas9/gRNAs, targeting mouse *Siglec15*, were generated by GenoMediTech (China) (Table S4).

Cell viability analysis

To examine the growth ability of transfected tumor cells, 5×10^3 cells of tested cell line were seeded in each well of a 96-well plate, which was then cultivated under condition of 37°C and 5% CO₂ for 48 h. Then solution of Cell Counting Kit-8 (BOSTER, AR1160) were diluted and added into cells of a 96-well plate according to the manufactured protocols. Light absorbance (OD450 minus OD600) was measured after 2 h incubation at 37°C, which was for further analysis of viability

difference between groups, and 3 time points were examined for each transfected cell line.

Construction of orthotopic and percutaneous mouse models

BALB/c nude (immunodeficient, RRID: IMSR_JAX:002019) and C57BL (immunocompetent, RRID: IMSR_ORNL:C57BL) male mice of 6–8 weeks old were used for tumor model construction in our investigation. 5 mice, fed with ordinary diet, were raised in one cage in specific pathogen free (SPF) environment. Huh7 (RRID: CVCL_0036, 1×10^6), MHCC97H (RRID: CVCL_4972, 1×10^6) and Hep1–6 (RRID: CVCL_0327, 2×10^5) cells were injected percutaneously into the right flank of BALB/c nude or C57BL mice to generate percutaneous tumor models. For construction of orthotopic liver tumor models, sliced Hep1–6 tumor tissue (1 mm^3) was surgically implanted into mouse liver after anesthesia.

To evaluate the treatment efficacy of anti-SIGLEC15 immunotherapy, eight days after percutaneous cell injection, SIGLEC15-blocking antibody (200 µg each) was intraperitoneally injected into each mice twice a week. Anti-SIGLEC15 antibody was generated by SanYou Biotech (China) according to related patterns.¹³ A caliper was used to measure the sizes of percutaneous tumors.

Extraction of tumor-infiltrated lymphocytes

Percoll solution (GE Health) was used to separate lymphocytes from tumor tissues according to the published protocols. Briefly, tumors were trimmed into 2 mm^3 pieces in dish before digestion (10 ml of solution with 0.1% DNase I and 0.1% collagenase IV).^{22,23} The mixed tissue solution was then incubated at 37°C for 30 min with a speed of 120 rounds/min for proper tissue digestion. Then, the mixed solution was applied to a gentle MACS dis-associator for further decomposition, which was set to the according grinding mode. After decomposition process, tubes with tissue solution were put on ice, and 10 ml of 2% FACS solution was added into each tube to neutralize tissue digestion enzymes; afterward, the mixed solution was filtered through a 70 µm mesh to get rid of the tissue debris. Centrifugation at 1500 rpm was performed to obtain cell pellets in filtered tissue solution, which was then further separated by Percoll solution at gradient dilutions of 30% and 70%. Cell pellets between 30% and 70% Percoll interface were mononuclear lymphocytes and could be collected and washed with cold PBS before further analysis.

Cell staining process and flow cytometry analysis

Extracted lymphocytes were allocated into 1.5 ml tubes (10^6 each) in 100 µl staining buffer (BioLegend). TruStain FcXtrade (BioLegend) was applied to block Fc receptors for 5 min at 4°C, and then antibodies for cell surface markers were added for staining process (4°C, 30 min). For intracellular staining, cell pellets, after surface marker staining process, were washed twice with cold staining buffer and then centrifuged at 1500 rpm; eBioscience Foxp3/Transcription Factor Staining Buffer Set (Invitrogen, Thermo Fisher Scientific) was

used for cell pellets fixation and permeabilization (1 h, room temperature) according to the manufactured protocols. Final cell pellets were then washed twice with fixation solution and suspended in 500 μ l staining buffer (BioLegend) for flow cytometry analysis on the BD FACS Aria III platform.

Co-culture system of tumor and Jurkat cell lines

To investigate the influences of SIGLEC15 expression on T cells, we constructed a co-culture system of tumor and Jurkat cells *in vitro*. Briefly, tumor cells were seeded into a 6-well plate for cultivation (37°C, 5% CO₂), and after 80% coverage of each cell was achieved, 1×10^5 Jurkat cells were added into the cell medium for co-culture of 48 h. Then floating cells in medium were collected through centrifugation at 1000 rpm. Collected cell pellets were stained for CD3 and GZMB expression for further flow cytometry analysis.

Magnetic sorting of immune cells

Anti-CD8a magnetic beads (StemCell) were used for enrichment of tumor-infiltrated CD8+ T cells, and anti-CD45 magnetic beads (StemCell) were used to enrich CD45+ lymphocytes for further single-cell sequencing analysis according to the manufactured protocols. Briefly, extracted lymphocytes were washed with cell medium and adapted to certain cell concentration. Then antibody cocktail in the kit was added into the cell medium according to the protocols, and cell solution was further mixed and incubated at room temperature for 5 min before adding the magnetic beads for another round of mixture and incubation for 3 min at room temperature. Finally, the tube, containing cell pellets, was placed into a magnet for incubation of 5 min. After pouring the unwanted cell pellets out, the enriched targeting cells were remained and could be reconstituted into certain concentration for further usage.

Single cell sequencing (scRNA-seq) and bulk sequencing analysis

Tumor cell suspension was incubated with anti-CD45 magnetic beads (StemCell) for lymphocyte enrichment. After that, CD45+ and CD45- cells were mixed at a ratio of 1:1 for further sequencing analysis on a 10 \times Genomics Platform with cell viability over 90%. A total of 17,100 cells were yielded in sequencing, and after filtering (percent.mt < 5%, nFeature < 2500 & > 200), 11,241 cells (IgG: 5765 cells, anti-SIGLEC15: 5482 cells) were remained for further analysis. Cell clusters were classified as lymphocytes and non-lymphocytes according to *Cd45* expression and annotated according to specific markers (Table S5). Magnetic enriched *CD8a* positive T cells from mouse tumor models were collected and prepared for total RNA extraction, which was further examined in quality control process and then loaded onto sequencing platform (DNB-seq). The yielded data were applied to following data filtration, and mapped genetic expressions were finally used in downstream analysis.

Monocytes depletion

To investigate whether tumor-derived SIGLEC15 expression was sufficient to induce immune evasion in tumor microenvironment, anionic clophosomes (BioLegend) were used to deplete mononuclear phagocytes in mouse model through percutaneous injection at a dose of 100 μ g per mouse. To consistently eradicate mononuclear phagocytes, anionic clophosome was injected twice a week. Clearance of mononuclear phagocytes in mouse tumors was confirmed by flow cytometry analysis through staining and gating CD11b and F4/80 positive cells.

Tumor tissue microarray (TMA)

Patient tumor samples were fixed in formaldehyde for 48 h and then embedded in wax. Afterwards, tissues were loaded and pinned onto glass plates with two points representing one sample. The aligned tissue array was then stored at 4°C for usage. A cohort of 221 HCC patients, who were treated in Zhongshan Hospital affiliated with Fudan University, Shanghai, China, were analyzed (Table S1).

Immunohistochemistry analysis (IHC)

Slides were incubated in Tris-EDTA buffer at 100°C for epitope retrieval. Then, intrinsic peroxidase activity was blocked for 15 min with 3% hydrogen peroxide at room temperature. Blocking buffer containing 5% bovine serum albumin was used for blockade for 30 min. Afterward, slides were incubated with primary antibodies at specific dilution ratios (anti-SIGLEC15, 1:400, NOVUS, Cat#NBP2-41162; anti-PD-L1, 1:30, Abcam, Cat#ab205921, RRID: AB_2687878) overnight in 4°C environment, followed by incubation with anti-rabbit or commonly used secondary antibodies for 60 min at room temperature. Diaminobenzidine chromogen substrate was used to detect antibody staining. Hematoxylin was used to counterstain the slides for 5 min after three washes with deionized water. Staining scores of each marker were analyzed by two independent physicians, according to staining areas and staining intensity, which were rated from point 0 to 4.

Bioinformatic analysis

HCC Sequencing data from the Cancer Genome Atlas (TCGA) and the International Cancer Genome Consortium (ICGC) databases were used for expression analysis.^{24–26} edgeR package (edgeR, RRID:SCR_012802) was used to examine differentially expressed genes between groups.^{27,28} The ggplot2 and Seurat packages were used for graphic demonstration.²⁹ Monocle package was used for trajectory analysis.^{30–32}

Ethical statement

All samples from patients, used in the investigation, were obtained with informed consent, which was approved by the local ethical committee of Zhongshan Hospital Ethical Review Board.

Statistics

Expression differences between two groups were examined with student t tests. Survival differences between groups were examined with the log-rank test. p values under .05 was considered significant.

Results

SIGLEC15 was negatively correlated with PD-L1 in HCC samples, relating an immune-barren microenvironment and unfavorable prognosis

We examined SIGLEC15 expression in databases and found that SIGLEC15 mRNA expression was increased in tumor samples, which was further confirmed by PCR analysis of paired HCC samples (Figure 1(a-c)). Further IHC analysis of 221 HCC patient tumor tissues (characteristics shown in Table S1) showed that SIGLEC15 protein expression in tumors was related to worse overall survival (OS) and disease-free survival (DFS) of patients (Figure 1(d-f)). We examined the correlation between SIGLEC15 expression and immune microenvironment characteristics through bioinformatic analysis, and we found mRNA expression of PD-L1 and SIGLEC15 in public HCC datasets (TCGA-LIHC, ICGC-LIRI) demonstrated polarized patterns: SIGLEC15-high samples turned to have lower expression of PD-L1, while PD-L1-high samples demonstrated fewer mRNA counts of SIGLEC15, with different genetic

profiles between sample groups (Figure 2a). Examination of differentially expressed genes between SIGLEC15-high and PD-L1-high samples demonstrated that immune-related cell and functional signatures were highly expressed in PD-L1 high samples, while SIGLEC15-high samples showed an immune-barren status in contrast (Figure 2b). We additionally examined IHC expression of PD-L1 in HCC patient cohort, in which 32.27% samples showed no expression of PD-L1 and high expression of SIGLEC15, while 27.73% samples were PD-L1 positive with low or none expression of SIGLEC15 (Figure 2(c-d)). Further examination of HCC cell lines also showed negatively correlated expression patterns between SIGLEC15 and PD-L1, and SIGLEC15 was relatively higher in HCC cell lines with aggressive traits (Figure 2e). In summary, SIGLEC15 was examined to negatively correlate with PD-L1 expression in HCC tumor samples, and SIGLEC15-high samples shared an immune-barren microenvironment with shorter overall survival and disease-free survival.

SIGLEC15 expressed by HCC tumor cells mainly promote tumor growth through evasion of cytotoxic CD8+ T cell killing

To explore whether SIGLEC15 expression could directly influence tumor growth, we knocked down SIGLEC15 in cell lines of MHCC97H and Huh7 (Supplemental Figure

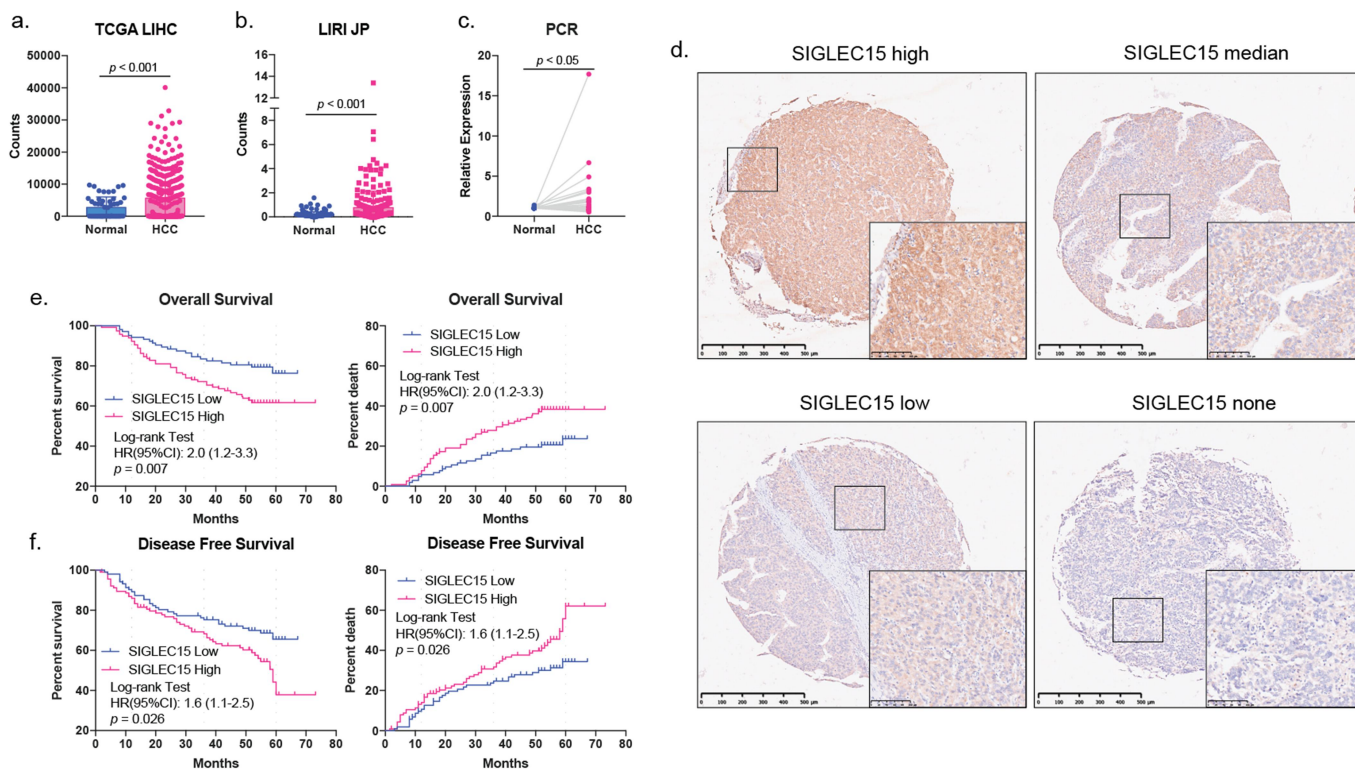


Figure 1. SIGLEC15 was highly expressed in HCC tumor samples and was related to deleterious survival of patients. a-c. Genetic expression of SIGLEC15 in public and local HCC tissue samples. (a. Expression counts of SIGLEC15 in TCGA-LIHC dataset showed SIGLEC15 expression was higher in HCC in contrast to normal liver samples; b. Expression counts of SIGLEC15 in ICGC-LIRI dataset showed SIGLEC15 was also highly expressed in HCC in comparison to normal liver tissues; c. PCR analysis of local HCC and paired normal tissues demonstrated that SIGLEC15 was highly expressed in tumor samples.) d. Representative SIGLEC15 expression images in IHC analysis of HCC tissue microarray. e-f. SIGLEC15 expression was related to deleterious overall survival and disease-free survival in IHC-examined HCC sample cohort ($n = 221$). (e. IHC analysis of examined HCC tissues showed high expression of SIGLEC15 was related to poor overall survival and high accumulative death rate; f. in calculation of disease-free survival and related accumulative death rate, high SIGLEC15 expression was also a significant risk factor in examined samples.)

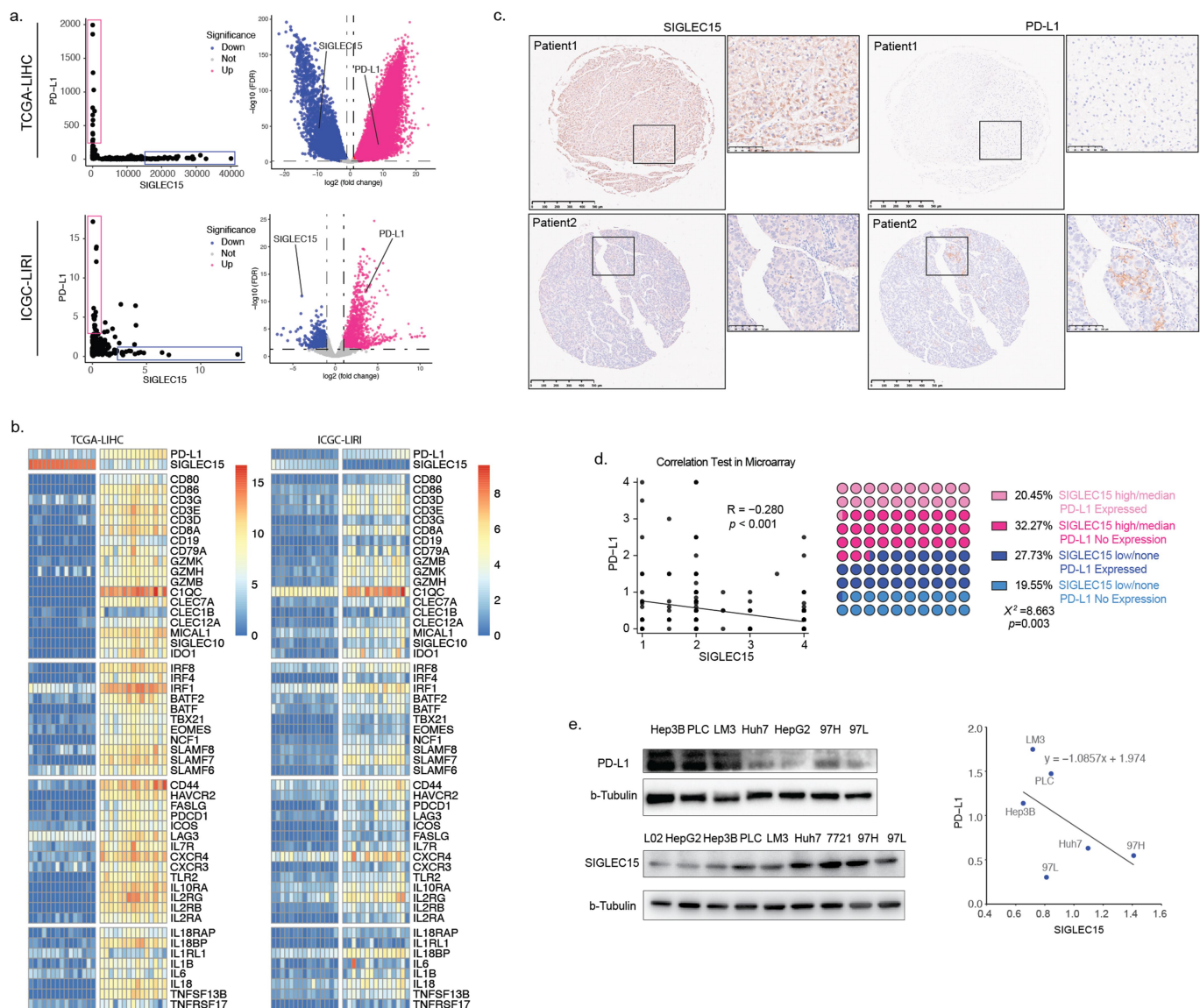


Figure 2. SIGLEC15 expression was negatively correlated with PD-L1 expression in HCC samples, relating to a barren immune microenvironment in tumor. **a.** Counts expression of SIGLEC15 and PD-L1 in HCC tumor samples demonstrated polarized expression patterns in public datasets of TCGA-LIHC and ICGC-LIRI, showing negative genetic correlations in data. **b.** Further examination of differentially expressed genes in polarized HCC samples demonstrated that samples with high expression of SIGLEC15 showed poor immune infiltration status across datasets of TCGA-LIHC and ICGC-LIRI, while samples with high expression of PD-L1 demonstrated an activated immune microenvironment with higher expression of immune-related markers. **c-d.** IHC examination of SIGLEC15 and PD-L1 also demonstrated a negative correlation in HCC samples. **c.** Representative images of negatively correlated SIGLEC15 and PD-L1 expression in HCC tumor samples; **d.** IHC staining scores for SIGLEC15 and PD-L1 demonstrated that tumor samples with high SIGLEC15 expression scores turned to present low levels of PD-L1 expression, and HCC samples examined in IHC analysis could be categorized into four groups according to SIGLEC15 and PD-L1 expression, in which samples classified as SIGLEC15 high/median and PD-L1 no-expression counted for 32.27% in total.) **e.** Examination of SIGLEC15 and PD-L1 expression in HCC cell lines additionally demonstrated negative correlation in expression.

S1a-c), and found decrease of SIGLEC15 expression in MHCC97H and Huh7 cells did not affect cell growth in vitro through CCK8 examination (Figure 3(a-b)). Also, in vivo analysis showed that knockdown of SIGLEC15 in tumor cells did not affect tumor growth in immune deficient mice (BALB/c nude) (Figure 3(c-d)). However, in immunocompetent C57 mice, knockout of *Siglec15* in Hep1-6 HCC tumor cells could significantly inhibit tumor growth in orthotopic and percutaneous tumor models (Figure 3(e-f)). Since mature and functional T cell populations are deficient in BALB/c nude mice, we wondered whether SIGLEC15 influenced cytotoxic T cells to promote tumor growth and constructed a co-culture system of HCC

and T cell lines (Figure 3g). We found SIGLEC15 knock-down in Huh7 cells could increase GZMB expression in Jurkat cells (CD3+) after co-culture of 48 h, while overexpression of SIGLEC15 could decrease GZMB expression in Jurkat cells accordingly (Figure 3(h-i)). We then examined tumor-infiltrating CD8+ T cells in mouse model and it demonstrated that knockout of *Siglec15* in Hep1-6 cells could restore CD8+ T cell cytotoxicity with increased expression of GZMB and IFN γ in tumor microenvironment (Figure 3(j-l)). In conclusion, SIGLEC15, expressed by tumor cells in HCC, mainly promoted malignancy growth through induction of CD8+ T cell anergy in tumor microenvironment.

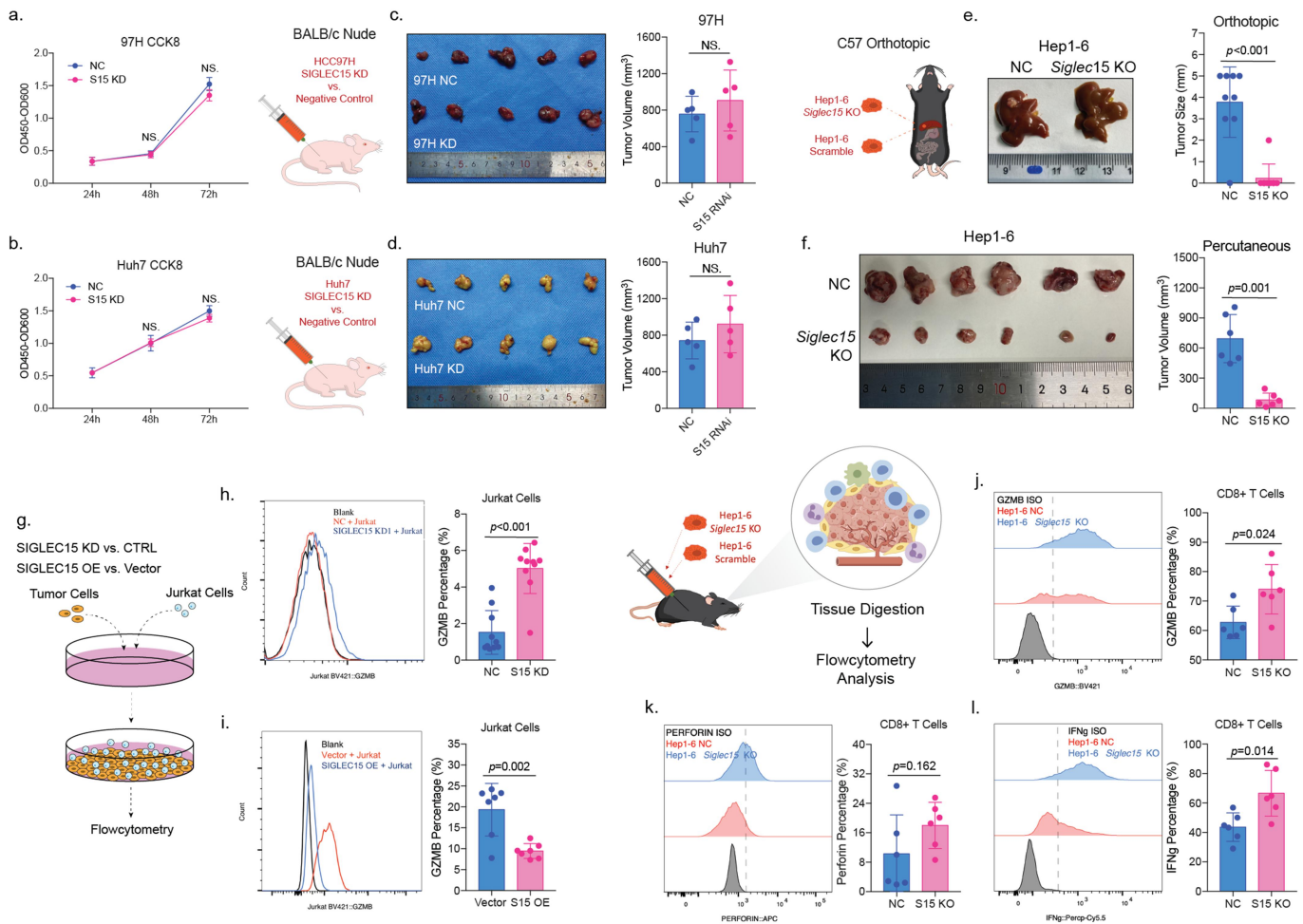


Figure 3. SIGLEC15, expressed by tumor cells, mainly promoted HCC growth through immune evasion. a-b. Cell viability analysis of SIGLEC15 knock-down HCC cell lines. (a. SIGLEC15 knock-down in MHCC97H cell models did not affect cell viability in CCK8 examination; b. SIGLEC15 knock-down in Huh7 cell models also did not influence cell growth examined by CCK8 tests.) c-d. Evaluation of subcutaneous tumor grafts in mature T cell deficient BALB/c nude mice ($n = 5$). (c. Evaluation of subcutaneous tumor growth of SIGLEC15 knock-down MHCC97H cells demonstrated that SIGLEC15 expression did not affect tumor growth in vivo without immune surveillance of T/B cells; d. Knock-down of SIGLEC15 in Huh7 cells also did not affect tumor growth ability in vivo without mature T cells.) e-f. Tumor growth evaluation of *Siglec15* knockout Hep1-6 cells in orthotopic ($n = 9$) and subcutaneous ($n = 6$) tumor models of immune competent C57 mice. (e. Knock-out of *Siglec15* in Hep1-6 cell line could inhibited tumor formation in liver of mouse orthotopic models with competent immune microenvironment; f. *Siglec15* knockout Hep1-6 tumor cells demonstrated impaired growth ability in comparison to control tumor cells injected subcutaneously in mice with normal immune activity.) g. Schematic demonstration of a tumor cell and T cell co-cultured system. h-i. SIGLEC15 expression in tumor cells could dampen cytotoxic function of Jurkat cells in vitro after co-culture of 48 h. (h. Co-cultured with SIGLEC15 knock-down Huh7 cells could increase GZMB expression in Jurkat cells through flow cytometry examination; i. Overexpression of SIGLEC15 in Huh7 tumor cells through plasmids transfection could reduce GZMB expression in Jurkat cells after co-culture.) j-l. Functional examination of CD8+ T cells in *Siglec15* knockout subcutaneous tumors. (j. *Siglec15* knockout in Hep1-6 cells could promote CD8+ T cell GZMB expression in tumor microenvironment of immune competent C57 mice; k. *Siglec15* knockout in Hep1-6 cells did not significantly increased perforin expression in CD8+ T cells in tumor in comparison to control models; l. Knock-out of *Siglec15* in Hep1-6 tumor cells could also increase IFNg expression in CD8+ T cells in subcutaneous tumor of immune competent C57 mouse models.)

Anti-SIGLEC15 treatment in HCC mouse model could reinvigorate CD8+ T cell cytotoxicity and inhibit tumor growth

We further applied SIGLEC15 antibody in subcutaneous HCC mouse models to investigate whether targeting SIGLEC15 in tumor could inhibit HCC growth in preclinical models (Figure 4a). We found anti-SIGLEC15 therapy could sufficiently reduce tumor volumes and prolong survival of tumor-bearing mice (Figure 4(b,f)). Analysis of tumor-infiltrating CD8+ T cells indicated anti-SIGLEC15 treatment significantly reinvigorated cytotoxic functions of CD8+ T cells in tumor, increasing GZMB and IFNg expression accordingly (Figure 4(c-e)). Former study demonstrated SIGLEC15, expressed by tumor associated

macrophages, could dampen functions of CD8+ T cells in melanoma, and we depleted mononuclear phagocytes, basically macrophages (F4/80+ and CD11b+), in mouse model to testify whether tumor-derived SIGLEC15 was crucial in immune evasion of HCC (Figure 4(g-h)). After depletion of mononuclear phagocytes, it showed anti-SIGLEC15 treatment still significantly inhibited tumor growth in comparison to IgG group, while simply depleting mononuclear phagocytes did not influence tumor growth in vivo (Figure 4(i-j)). So, tumor-derived SIGLEC15 expression was sufficient to induce immune evasion in HCC, and anti-SIGLEC15 treatment in preclinical HCC mouse models could reinvigorate cytotoxic CD8+ T cells to inhibit tumor growth.

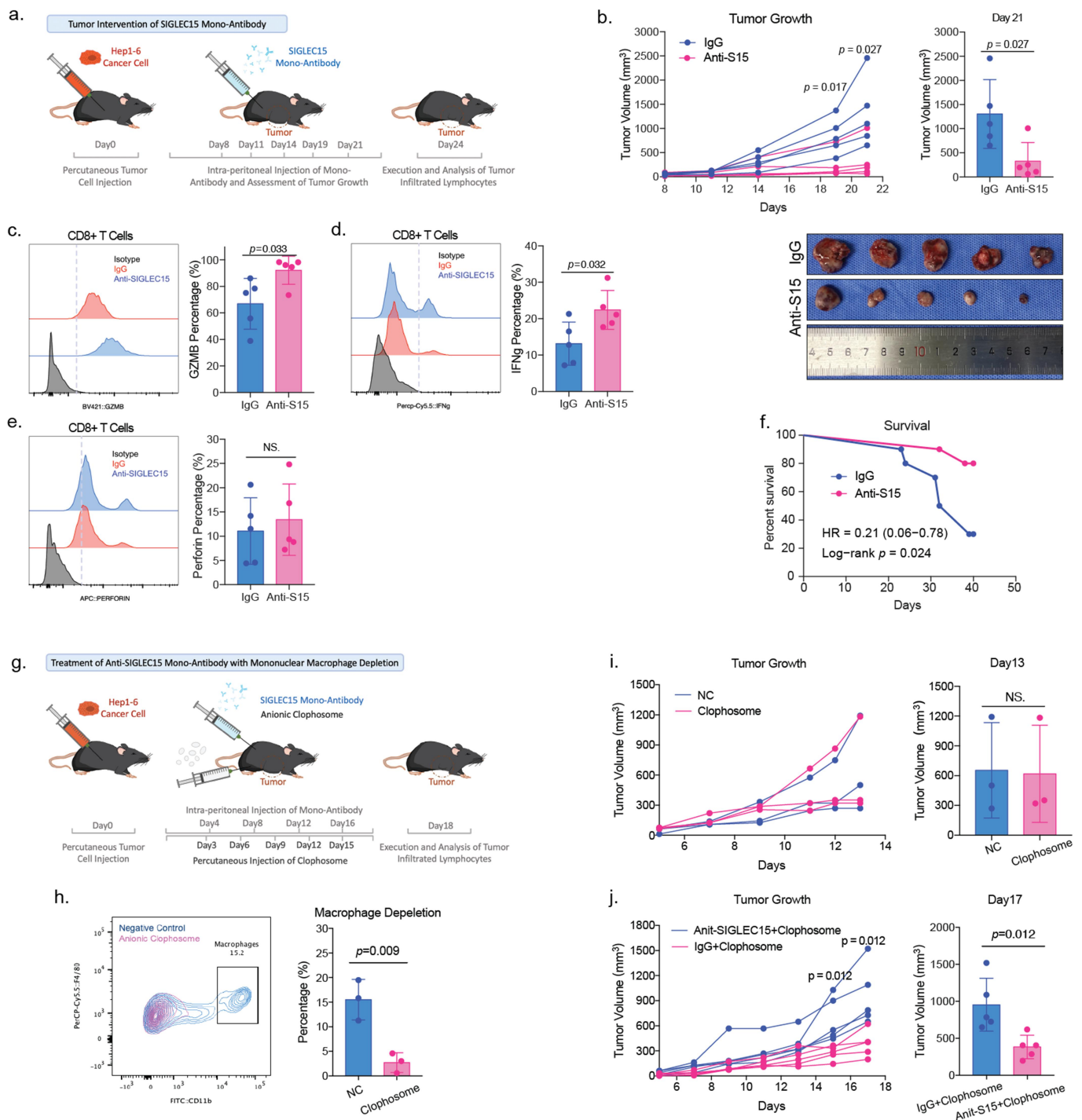


Figure 4. Anti-SIGLEC15 immunotherapy could reduce tumor burden and promote CD8+ T cell cytotoxic functions in mouse models. a. Schematic demonstration of anti-SIGLEC15 treatment in subcutaneous tumor models of C57 mice. b. Anti-SIGLEC15 treatment inhibited subcutaneous tumor growth ($n = 5$). c-e. Anti-SIGLEC15 therapy could reinvigorate cytotoxic CD8+ T cell functions in tumor. (c. Anti-SIGLEC15 treatment increased GZMB expression in CD8+ T cells in tumor examined by flow cytometry; d. IFN γ expression in CD8+ T cells was also increased after anti-SIGLEC15 treatment; e. Difference of perforin expression in CD8+ T cells was not observed between tumor-bearing mice with or without anti-SIGLEC15 treatment.) f. Anti-SIGLEC15 treatment improved survival of tumor bearing mice ($n = 10$). g. Schematic demonstration of macrophage deletion in addition to anti-SIGLEC15 therapy in C57 HCC mouse models. h. Mononuclear phagocyte depletion in C57 mice ($n = 3$) with anionic clophosome (100ul per mouse) could significantly reduce corresponding cell populations. i. Clearance of mononuclear phagocytes did not influence tumor growth in vivo ($n = 3$). j. Anti-SIGLEC15 treatment could still significantly inhibit tumor growth in mouse model after macrophage depletion ($n = 5$).

SIGLEC15 could induce infiltrated CD8+ T cell apoptosis in HCC tumor microenvironment

We examined CD8+ T cell portions between anti-SIGLEC15 and IgG treatment groups, and we found anti-SIGLEC15 treatment could increase CD8+ T cell infiltration in HCC tumor model

(Figure 5a). It turned out that CD8+ T cell infiltrating levels were negatively correlated with tumor burden in mouse models (Figure 5b). To understand how SIGLEC15 affected CD8+ T cells in HCC tumor microenvironment, we additionally collected magnetically enriched CD8+ T cells in tumor tissues for sequencing analysis. Differentially expressed genes between

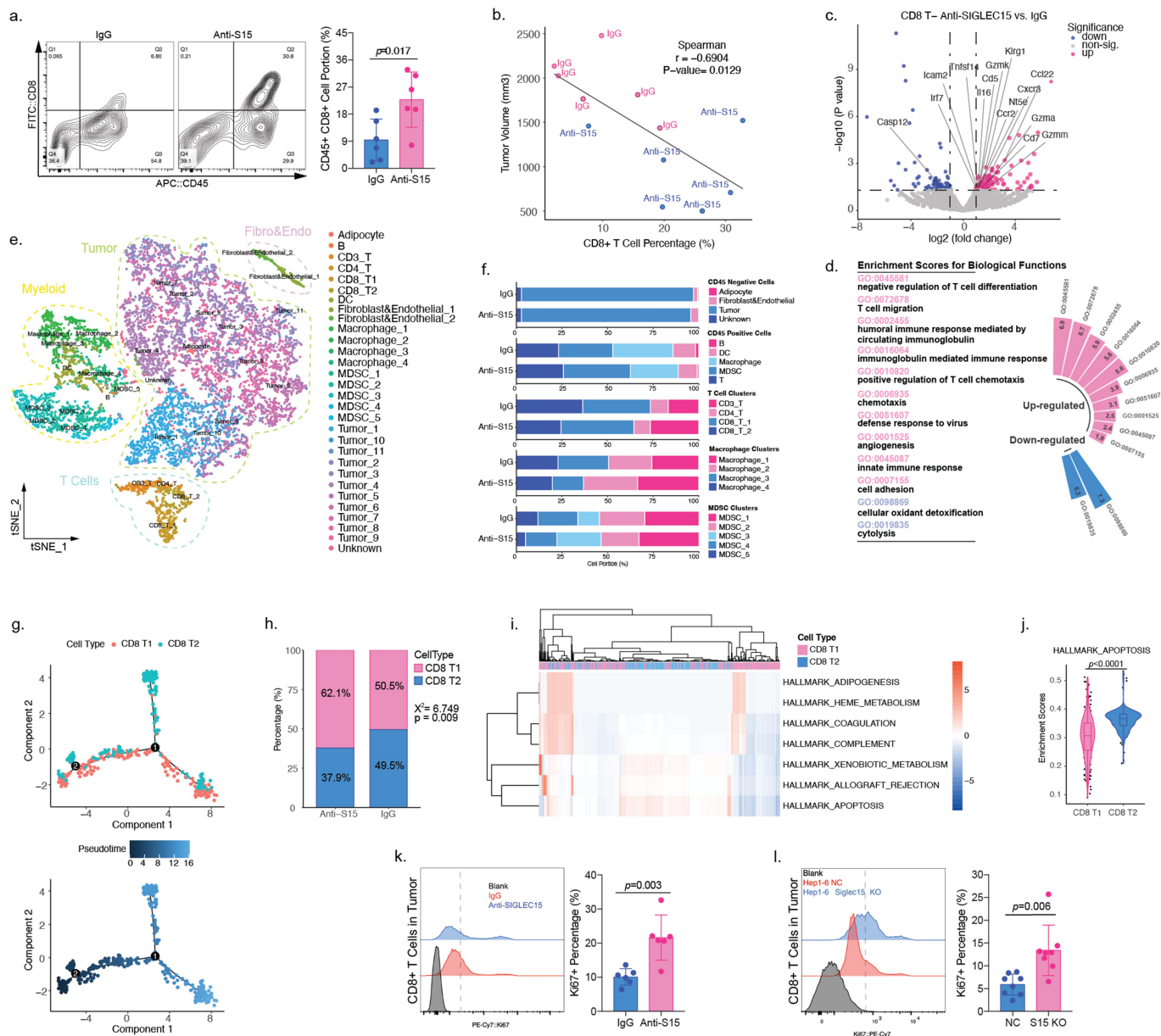


Figure 5. SIGLEC15 could induce CD8+ T cell apoptosis in HCC tumor microenvironment. a. Anti-SIGLEC15 could increase CD8+ T cell infiltration in HCC tumor microenvironment through flow cytometry examination. b. CD8+ T cell portions were negatively correlated with tumor volume in mouse models. c. Transcriptional difference in magnetically enriched CD8+ T cells of mouse tumors between groups of anti-SIGLEC15 and IgG treatment. d. Biological function annotation of differentially expressed genes showed anti-SIGLEC15 treatment could promote T cell migration and chemotaxis. e-f. scRNA-seq analysis of C57 mouse subcutaneous tumor grafts treated by IgG and anti-SIGLEC15 antibody. (e. Annotated cell clusters of tumor samples after filtration; f. Portions of major cell clusters in tumor samples treated by IgG or anti-SIGLEC15 antibody.) g. Developmental trajectories of CD8+ T cell clusters in tumor demonstrated that main CD8 T2 cluster cells shared a different development trajectory in contrast to CD8 T1 cluster cells. h. Anti-SIGLEC15 treatment could reduce CD8 T2 cluster cells in mouse tumors. i. Signaling analysis of CD8+ T cell clusters in tumor model demonstrated that various signals were differently expressed between CD8 T1 and CD8 T2 clusters, emphasizing different T cell status. j. Among the selected signals, CD8 T1 cluster had lower apoptotic signaling in comparison to CD8 T2 cluster. k-l. Anti-SIGLEC15 or *Siglec15* knockout in tumor cell could both increase Ki67 expression in CD8+ T cells in tumor microenvironment. (k. Flow cytometry analysis of Ki67 expression in CD8+ T cells from IgG and anti-SIGLEC15 antibody treated C57 subcutaneous tumors demonstrated anti-SIGLEC15 treatment could increase Ki67 expression in CD8+ T cells; l. Knock-out *Siglec15* in Hep1-6 cells could also increase Ki67 expression in CD8+ T cells in tumor microenvironment).

groups (anti-SIGLEC15 vs. IgG) were enriched for further annotation, and it demonstrated that CD8+ T cells were highly activated and mobile after anti-SIGLEC15 treatment, while apoptotic signatures were down-regulated, such as *Casp12* (Figure 5(c-d)). We additionally performed scRNA-seq analysis of mouse tumor samples (anti-SIGLEC15 vs. IgG), and finally 11,247 cells were yielded after cell filtration for downstream analysis (Figure 5e); anti-SIGLEC15 treatment mainly influenced T cell and myeloid cell cluster portions between groups

(Figure 5f). We wondered how CD8+ T cells changed after deletion of SIGLEC15 signals and performed trajectory analysis accordingly. It appeared CD8 T2 cluster took a single arm in CD8+ T cell developmental trajectories; also, anti-SIGLEC15 could alter CD8+ T cell trajectories by increasing CD8 T1 and reducing CD8 T2 cell portions in the process (Figure 5(g-h)). Analysis of signaling changes between CD8+ T cell clusters demonstrated that the apoptotic signaling was significantly lower in CD8 T1 cluster (Figure 5(i-j)). We further examined

cell viability of tumor infiltrated CD8+ T cells through examination of Ki67 expression and found *Siglec15* knockout or anti-SIGLEC15 treatment could both increase CD8+ T cell viability in tumor (Figure 5(k-l)). In summary, SIGLEC15 could induce CD8+ T cell apoptosis to promote immune evasion in HCC, and anti-SIGLEC15 treatment could modify CD8+ T cell developmental trajectories in HCC tumor model, increasing CD8+ T cell viability, promoting CD8+ T cell tumor infiltration and reinvigorate CD8+ T cell cytotoxicity at the same time.

Discussion

In our investigation, we found that SIGLEC15, expressed by HCC tumor cells, mainly promoted malignancy growth through immune evasion, inhibiting cytotoxicity and viability of CD8+ T cells in tumor microenvironment; SIGLEC15 expression levels in HCC tumor cells did not directly influence tumor cell viability. However, in a study concerning anaplastic thyroid carcinoma, knockout of *Siglec15* could reduce expression of STAT1, STAT3 and VEGF in tumor, leading to tumor cell apoptosis and reduced tumor volume.³³ Former studies demonstrated that SIGLEC15 were found to be expressed in macrophages and dendritic cells, which mainly regulate cell functions through downstream regulation of DAP12 and DAP10,³⁴ and in differentiated myeloid cells, such as osteoclasts, SIGLEC15 was examined to function with DAP12 in maintenance of osteoclast physiological functions.³⁵ The explicit roles of SIGLEC15 in tumor may vary according to different tissue origins, and our results demonstrated that in HCC, SIGLEC15 expression in tumor cell mainly promote tumor progression through immune evasion.

Studies showed that in melanoma and pancreatic adenocarcinoma tumor microenvironment, SIGLEC15 associated macrophages were polarized to induce CD8+ T cell dysfunction;^{13,36} we wonder if SIGLEC15-associated macrophages took the primal immune editing roles in CD8+ T cell dysfunction and delete mononuclear phagocytes in anti-SIGLEC15 treated mouse models accordingly. Our results showed anti-SIGLEC15 treatment still significantly inhibited tumor growth even after deletion of mononuclear phagocytes, emphasizing the crucial immunoregulatory function of SIGLEC15 in HCC tumor cells.

PD-L1 expression is an important indicator of immunotherapy efficacy across cancer types,³⁷ and a series of studies demonstrated that combination therapy could increase treatment responses through up-regulation of PD-L1 in tumor microenvironment.³⁸ In our investigation, SIGLEC15 expression was found negatively correlated with PD-L1 in HCC cell lines and tumor samples. SIGLEC15 mRNA was also found negatively correlated with PD-L1 in public melanoma sequencing data, and in a study concerning non-small-cell lung carcinoma (NSCLC), SIGLEC15 expression was higher in adenocarcinoma samples, while on the other hand, PD-L1 positive rate was higher in samples of squamous cell carcinoma.^{13,39} In various solid tumors, high expression of SIGLEC15 in malignancy or macrophages was all related to poor survival of patients, providing rationale for SIGLEC15-targeting

therapy in cancer patients,^{36,40} and preliminary results from an ongoing clinical trial indicated that anti-SIGLEC15 therapy achieved prolonged stabilization of disease in 54% (20/37) of recruited cancer patients, and in 20% (2/10) anti-PD1-refractory NSCLC patients, objective responses were observed.¹⁵ In our examined HCC patient cohort, 27% (61/221) samples demonstrated expression of PD-L1 and low/none expression of SIGLEC15, while 32% (71/221) patients showed high expression of SIGLEC15 and no expression of PD-L1, who may be potential candidates for anti-SIGLEC15 immunotherapy.

There are several limitations of our study. First, the examination of SIGLEC15 expression in HCC tumor samples was only performed in a small cohort of Chinese patients from a single center, which may not represent the overall characteristics of patients. Second, our results mainly relied on cell and mouse models, which may not replicate actual tumor microenvironment that develop over a long period of time in human.

Conclusion

SIGLEC15 was negatively correlated with PD-L1 expression in HCC and could promote tumor immune evasion through induction of CD8+ T cell apoptosis, relating to an immune barren tumor microenvironment.

Author contribution

ZC, MCH, QHY, LG and HL designed the investigation, and ZC, MCY, BZ, LJ, QY, SL, BHZ, JLY, WTZ and XQL conducted experiments of the study. ZC, MCY and BZ drafted the manuscript, and JZ, JF, YFX, YSX, MCH, QHY, LG and HL helped to revise and make adaptations. MCH, QHY, LG and HL administered the project. All authors are responsible for the content of the investigation.

Disclosure statement

No potential conflict of interest was reported by the author(s).

Funding

This work was funded by National Nature Science Foundation of China [82272774, 82102959, 82172739, 81871924, 82072666 and 81972829], Shanghai Natural Science Foundation [21ZR1481900], Beijing Xisike Clinical Oncology Research Foundation [Y-Roche2019/2-0037], Zhongshan Talent Development Program [2021ZSYQ11], China Postdoctoral Science Foundation Funded Project (2023M730652), and Zhongshan Hospital Funded Program (2024ZYYS-020).

Data availability statement

Sequencing data for the manuscript were deposited in the Gene Expression Omnibus database under the accession number of GSE218411. Public datasets of LIHC and LIRI projects were downloaded from TCGA and ICGC databases respectively. There was no original code generated in the manuscript.

References

- Bray F, Ferlay J, Soerjomataram I, Siegel RL, Torre LA, Jemal A. Global cancer statistics 2018: GLOBOCAN estimates of incidence and mortality worldwide for 36 cancers in 185 countries. *CA Cancer J Clin.* 2018;68(6):394–424. doi:10.3322/caac.21492.
- Singal AG, Lampertico P, Nahon P. Epidemiology and surveillance for hepatocellular carcinoma: new trends. *J Hepatol.* 2020;72(2):250–261. doi:10.1016/j.jhep.2019.08.025.
- Jindal A, Thadi A, Shailubhai K. Hepatocellular carcinoma: etiology and current and future drugs. *J Clin Exp Hepatol.* 2019;9(2):221–232. doi:10.1016/j.jceh.2019.01.004.
- Cheng AL, Hsu C, Chan SL, Choo SP, Kudo M. Challenges of combination therapy with immune checkpoint inhibitors for hepatocellular carcinoma. *J Hepatol.* 2020;72(2):307–319. doi:10.1016/j.jhep.2019.09.025.
- Meric-Bernstam F, Larkin J, Tabernero J, Bonini C. Enhancing anti-tumour efficacy with immunotherapy combinations. *Lancet.* 2021;397(10278):1010–1022. doi:10.1016/S0140-6736(20)32598-8.
- Upadhaya S, Neftelino ST, Hodge JP, Oliva C, Campbell JR, Yu JX. Combinations take centre stage in PD1/PDL1 inhibitor clinical trials. *Nat Rev Drug Discov.* 2021;20(3):168–169. doi:10.1038/d41573-020-00204-y.
- El-Khoueiry AB, Sangro B, Yau T, Crocenzi TS, Kudo M, Hsu C, Kim TY, Choo S-P, Trojan J, Welling TH, et al. Nivolumab in patients with advanced hepatocellular carcinoma (CheckMate 040): an open-label, non-comparative, phase 1/2 dose escalation and expansion trial. *Lancet.* 2017;389(10088):2492–2502. doi:10.1016/S0140-6736(17)31046-2.
- Yau T, Kang YK, Kim TY, El-Khoueiry AB, Santoro A, Sangro B, Melero I, Kudo M, Hou M-M, Matilla A, et al. Efficacy and safety of nivolumab plus ipilimumab in patients with advanced hepatocellular carcinoma previously treated with Sorafenib: the CheckMate 040 randomized clinical trial. *JAMA Oncol.* 2020;6(11):e204564. doi:10.1001/jamaoncol.2020.4564.
- Edner NM, Carlesso G, Rush JS, Walker LSK. Targeting co-stimulatory molecules in autoimmune disease. *Nat Rev Drug Discov.* 2020;19(12):860–883. doi:10.1038/s41573-020-0081-9.
- John P, Wei Y, Liu W, Du M, Guan F, Zang X. The B7x immune checkpoint pathway: from discovery to clinical trial. *Trends Pharmacol Sci.* 2019;40(11):883–896. doi:10.1016/j.tips.2019.09.008.
- Li J, Lee Y, Li Y, Jiang Y, Lu H, Zang W, Zhao X, Liu L, Chen Y, Tan H, et al. Co-inhibitory molecule B7 superfamily member 1 expressed by tumor-infiltrating myeloid cells induces dysfunction of anti-tumor CD8(+) T cells. *Immunity.* 2018;48(4):773–786.e5. doi:10.1016/j.immuni.2018.03.018.
- Peuker K, Strigli A, Tauriello DVF, Hendricks A, von Schönfels W, Burmeister G, Brosch M, Herrmann A, Krüger S, Nitsche J, et al. Microbiota-dependent activation of the myeloid calcineurin-NFAT pathway inhibits B7H3- and B7H4-dependent anti-tumor immunity in colorectal cancer. *Immunity.* 2022;55(4):701–717.e7. doi:10.1016/j.immuni.2022.03.008.
- Wang J, Sun J, Liu LN, Flies DB, Nie X, Toki M, Zhang J, Song C, Zarr M, Zhou X, et al. Siglec-15 as an immune suppressor and potential target for normalization cancer immunotherapy. *Nat Med.* 2019;25(4):656–666. doi:10.1038/s41591-019-0374-x.
- van de Wall S, Santeogoets KCM, van Houtum EJH, Büll C, Adema GJ. Sialoglycans and siglecs can shape the tumor immune microenvironment. *Trends Immunol.* 2020;41(4):274–285. doi:10.1016/j.it.2020.02.001.
- Sun J, Lu Q, Sanmamed MF, Wang J. Siglec-15 as an emerging target for next-generation cancer immunotherapy. *Clin Cancer Res.* 2021;27(3):680–688. doi:10.1158/1078-0432.CCR-19-2925.
- Bordon Y. Inflammation: live long and prosper with Siglecs. *Nat Rev Immunol.* 2015;15(5):266–267. doi:10.1038/nri3851.
- Zheng M, Tian ZG. Liver-mediated adaptive immune tolerance. *Front Immunol.* 2019;10:2525. doi:10.3389/fimmu.2019.02525.
- Lu LC, Hsu C, Shao YY, Chao Y, Yen CJ, Shih IL, Hung YP, Chang C-J, Shen Y-C, Guo J-C, et al. Differential organ-specific tumor response to immune checkpoint inhibitors in hepatocellular carcinoma. *J Liver Cancer.* 2019;8(6):480–490. doi:10.1159/000501275.
- Nault JC, Villanueva A. Biomarkers for hepatobiliary cancers. *Hepatology.* 2021;73(Suppl 1):115–127. doi:10.1002/hep.31175.
- Ally A, Balasundaram M, Carlsen R, Chuah E, Clarke A, Dhalla N, Holt RA, Jones SJM, Lee D, Ma Y, et al. Comprehensive and integrative genomic characterization of hepatocellular carcinoma. *Cell.* 2017;169(7):1327–1341.e23. doi:10.1016/j.cell.2017.05.046.
- Racanelli V, Rehermann B. The liver as an immunological organ. *Hepatology.* 2006;43(Supplement 1):S54–62. doi:10.1002/hep.21060.
- Haubruck P, Colbath AC, Liu Y, Stoner S, Shu C, Little CB. Flow cytometry analysis of immune cell subsets within the murine spleen, bone marrow, lymph nodes and synovial tissue in an osteoarthritis model. *J Vis Exp.* 2020;(158). doi:10.3791/61008-v.
- Shi W, Wang Y, Zhang C, Jin H, Zeng Z, Wei L, Tian Y, Zhang D, Sun G. Isolation and purification of immune cells from the liver. *Int Immunopharmacol.* 2020;85:106632. doi:10.1016/j.intimp.2020.106632.
- Sun Y, Wu L, Zhong Y, Zhou K, Hou Y, Wang Z, Zhang Z, Xie J, Wang C, Chen D, et al. Single-cell landscape of the ecosystem in early-relapse hepatocellular carcinoma. *Cell.* 2021;184(2):404–421.e16. doi:10.1016/j.cell.2020.11.041.
- Hudson TJ, Anderson W, Aretz A, Barker AD, Bell C, Bernabé RR, Bhan MK, Calvo F, Eerola I, Gerhard, DS, Guttmacher A, et al. International network of cancer genome projects. *Nature.* 2010;464:993–998.
- Tomczak K, Czerwinska P, Wiznerowicz M. The Cancer Genome Atlas (TCGA): an immeasurable source of knowledge. *Contemp Oncol (Pozn).* 2015;19:A68–77. doi:10.5114/wo.2014.47136.
- Robinson MD, McCarthy DJ, Smyth GK. edgeR: a bioconductor package for differential expression analysis of digital gene expression data. *Bioinformatics.* 2010;26(1):139–140. doi:10.1093/bioinformatics/btp616.
- McCarthy DJ, Chen Y, Smyth GK. Differential expression analysis of multifactor RNA-Seq experiments with respect to biological variation. *Nucleic Acids Res.* 2012;40(10):4288–4297. doi:10.1093/nar/gks042.
- Stuart T, Butler A, Hoffman P, Hafemeister C, Papalexi E, Mauck WM 3rd, Hao Y, Stoeckius M, Smibert P, Satija R. Comprehensive integration of single-cell data. *Cell.* 2019;177(7):1888–1902.e21. doi:10.1016/j.cell.2019.05.031.
- Trapnell C, Cacchiarelli D, Grimsby J, Pokharel P, Li S, Morse M, Lennon NJ, Livak KJ, Mikkelsen TS, Rinn JL, et al. The dynamics and regulators of cell fate decisions are revealed by pseudotemporal ordering of single cells. *Nat Biotechnol.* 2014;32(4):381–386. doi:10.1038/nbt.2859.
- Qiu X, Hill A, Packer J, Lin D, Ma YA, Trapnell C. Single-cell mRNA quantification and differential analysis with Census. *Nat Methods.* 2017;14(3):309–315. doi:10.1038/nmeth.4150.
- Qiu X, Mao Q, Tang Y, Wang L, Chawla R, Pliner HA, Trapnell C. Reversed graph embedding resolves complex single-cell trajectories. *Nat Methods.* 2017;14(10):979–982. doi:10.1038/nmeth.4402.
- Hou X, Chen C, He X, Lan X. Siglec-15 silencing inhibits cell proliferation and promotes cell apoptosis by inhibiting STAT1/STAT3 signaling in anaplastic thyroid carcinoma. *Dis Markers.* 2022;2022:1606404. doi:10.1155/2022/1606404.
- Angata T, Tabuchi Y, Nakamura K, Nakamura M. Siglec-15: an immune system Siglec conserved throughout vertebrate evolution. *Glycobiology.* 2007;17(8):838–846. doi:10.1093/glycob/cwm049.
- Ishida-Kitagawa N, Tanaka K, Bao X, Kimura T, Miura T, Kitaoka Y, Hayashi K, Sato M, Maruoka M, Ogawa T, et al. Siglec-15 protein regulates formation of functional osteoclasts in concert with DNAX-activating protein of 12 kDa (DAP12). *J Biol Chem.* 2012;287(21):17493–17502. doi:10.1074/jbc.M111.324194.
- Li TJ, Jin KZ, Li H, Ye LY, Li PC, Jiang B, Lin X, Liao Z-Y, Zhang H-R, Shi S-M, et al. SIGLEC15 amplifies

- immunosuppressive properties of tumor-associated macrophages in pancreatic cancer. *Cancer Lett.* 2022;530:142–155. doi:10.1016/j.canlet.2022.01.026.
37. Doroshov DB, Bhalla S, Beasley MB, Sholl LM, Kerr KM, Grnjatic S, Wistuba II, Rimm DL, Tsao MS, Hirsch FR. PD-L1 as a biomarker of response to immune-checkpoint inhibitors. *Nat Rev Clin Oncol.* 2021;18(6):345–362. doi:10.1038/s41571-021-00473-5.
38. Yu M, Chen Z, Zhou Q, Zhang B, Huang J, Jin L, Zhou B, Liu S, Yan J, Li X, et al. PARG inhibition limits HCC progression and potentiates the efficacy of immune checkpoint therapy. *J Hepatol.* 2022;77(1):140–151. doi:10.1016/j.jhep.2022.01.026.
39. Hao JQ, Nong JY, Zhao D, Li HY, Su D, Zhou LJ, Dong YJ, Zhang C, Che NY, Zhang SC, et al. The significance of Siglec-15 expression in resectable non-small cell lung cancer. *Neoplasma.* 2020;67(6):1204–1222. doi:10.4149/neo_2020_200220N161.
40. Quirino MWL, Pereira MC, Deodato de Souza MF, Pitta IDR, Da Silva Filho AF, Albuquerque MSS, Albuquerque APB, Martins MR, Pitta MGDR, Rêgo MJBDM, et al. Immunopositivity for Siglec-15 in gastric cancer and its association with clinical and pathological parameters. *Eur J Histochem.* 2021;65(1):65. doi:10.4081/ejh.2021.3174.